

AN EMPIRICAL LOW-ENERGY ION MODEL OF THE INNER MAGNETOSPHERE

J. L. Roeder

The Aerospace Corporation
MS M2-260, P. O. Box 92957, Los Angeles, CA
310-336-7081

E-mail: James.Roeder@aero.org

M. W. Chen

J. F. Fennell

The Aerospace Corporation

R. Friedel

Los Alamos National Laboratory

Abstract

Ion flux measurements by the CAMMICE/MICS and Hydra instruments on the NASA Polar satellite have been used to build empirical models of the ion environment at low energies in the Earth's inner magnetosphere. These models may be used to develop design and test specifications for spacecraft surface materials, which are susceptible to damage by the ions. The combination of the CAMMICE/MICS and Hydra models provide the ion flux at energies in the range 20 eV–200 keV as a function of position in the magnetosphere. For the 1–200 keV energy range, the H⁺ and O⁺ ion flux is estimated separately using the CAMMICE/MICS data. Average environments have been calculated for several sample orbital trajectories: a geosynchronous orbit and the orbits of several satellites in the Global Positioning System (GPS) constellation. At high energies (~100 keV) the flux estimates agree with corresponding estimates from the NASA AP-8 model, but the fluxes at low energies are larger than those extrapolated simply from AP-8. The CAMMICE/MICS model shows that H⁺ dominates the >2 keV ion populations, but that the O⁺ flux becomes comparable to the H⁺ flux at ~1 keV. The standard deviation of both the ion and electron flux was found to be 100–200% of the average value over the entire considered energy range. The average 1–200 keV O⁺ flux estimates for GEO appear very similar to the averages for GPS orbit, so that any material damage due to O⁺ ions in this energy range should be the same for the two orbits.

Introduction

The impact of charged particles from the space environment can have substantial effects on the parts and materials used in space systems. The most well known is the gradual degradation of microelectronic devices by relatively high-energy (>100 keV) particles in the Earth's radiation belts. But lower energy particles also significantly damage materials at their outer surfaces. The effects include the collisional ejection of atoms of the material (sputtering), implantation of incident ions in the material, and chemical changes in the material due to those implanted ions [Johnson, 1990; Nastasi, 1996]. These processes become especially important for the design of optical and thermal coatings for the satellite surface. Such coatings rely on precisely known properties of the material surface to remain within specification over the mission lifetime.

Effects such as sputtering occur very gradually over the space mission but the damage is cumulative, similar to the total dose radiation effects on microelectronics. Because of this, the relevant specification for the environment is the average flux of particles as a function of incident energy over the entire mission. This spectrum may then be converted to a profile of dose versus depth that is related to the damage of the material.

The charged particles in the space environment consist of electrons and ions of various masses and charge states. Higher mass particles tend to be more effective at a given energy for damaging the surface of materials, so the flux of ions of each species is important for estimating these effects. The range of ion energy that is important for material surface damage is quite uncertain. It depends on many factors including incident angle, material properties, and particle mass. In broad terms, ions of energy in the range from ~ 100 eV to ~ 100 keV are important for surface effects. The electrons in this energy range may cause little surface damage to materials but result in other important effects such as the surface charging of dielectric materials [Hastings and Garrett, 1996].

The NASA radiation belt models such as AE8 and AP8 are traditionally used to specify the average charged-particle flux for space missions [Vette, 1991]. But these models cover the energy range of 0.04–10 MeV for electrons and 0.1–10 MeV for protons. The particles in these ranges are too energetic to cause significant damage to the surface of spacecraft materials, and will instead burrow deep in to the spacecraft. Extrapolation of the NASA models to low energies is too uncertain for use as an environmental specification, and so a low-energy particle model is needed for space system design.

In this report we present a model of charged particles in the energy range 20 eV–200 keV that we have constructed using particle observations by the recent NASA Polar satellite. The model consists of the average flux for the major ion species as a function of the three-dimensional position in the Earth's magnetosphere. Similar to the NASA models, one can then “fly” a spacecraft through the model and determine the average environment along the trajectory. We use the model to determine the average particle environment for spacecraft in both geosynchronous orbit and a representative orbit of the Global Positioning System (GPS). The results are compared with the NASA AP8 and AE8 and other published models.

Instrumentation

Polar is a NASA satellite mission to investigate the Earth's magnetosphere [Acuna et al., 1995]. It is part of the Global Geospace Science program that is designed to improve understanding of the flow of energy, mass, and momentum in the solar-terrestrial environment. The Polar spacecraft was launched on February 26, 1996 into a 1.8 x 9 RE orbit with a 90° inclination and an 18-hour period. The spacecraft has both spinning and de-spun platforms for instruments. All the instrumentation described in this report were mounted on the spinning platform which has a spin period of ~ 6 s. The spin axis pointed nearly perpendicular to the orbit plane so that the satellite cartwheeled along the orbit.

Data from two instruments on the Polar satellite were used to construct a model of the charged particle environment. The Magnetospheric Ion Composition Spectrometer (MICS) was

part of the Charge and Mass Magnetospheric Ion Composition Experiment (CAMMICE) on the Polar satellite. MICS measured all positively charged ion species ranging in mass from hydrogen to iron in the energy-per-charge range 1–200 keV/q. This sensor was similar to an identically named instrument on the USAF/NASA CRRES mission [Wilken et al., 1992].

MICS determined the identity of each detected ion from three measurements: the energy-per-charge (E/q), the time-of-flight (TOF) for the ion to traverse a fixed distance, and a total energy (E). The detection events were then sorted by a data processing unit for accumulation into bins for the various ion mass species and charge states [Koga et al., 1992]. The major ion species (H, He, and O) in the magnetosphere each had a low and a high-energy channel. The high-energy channel required a valid energy measurement in addition to the TOF and E/q , and was able to unambiguously determine the ion charge state. The low energy channel required only TOF and E/q measurements and was thus insensitive to the ion charge state. Inside the Earth's magnetosphere the particle populations are heavily dominated by singly charged ions, so the low energy channels are assumed to represent ions of charge state one. The data from the low and high-energy channels may then be combined into a composite spectrum in the range 1–200 keV. The hydrogen and oxygen ion spectra in this report are all composite measurements constructed by this process. A total ion channel is also recorded which counts ions irrespective of mass or charge state. Data from this channel is assumed to be protons.

MICS measured the ion flux in 24 logarithmically-spaced steps over the range 1–200 keV/q. The instrument was programmed to provide a full-resolution energy spectrum every 202 s. The MICS sensor had a single field-of-view directed perpendicular to the spacecraft spin axis. Ion counts were accumulated in 32 equally-space sectors for each spacecraft spin period, which effectively limited the angular resolution to $\sim 11.25^\circ$.

The CAMMICE/MICS data was supplemented by measurements from the Hydra instrument, also on the Polar mission. Hydra measured ion and electron flux in the energy-per-charge range 2 eV/q–35 keV/q [Scudder et al., 1995]. This instrument had multiple fields-of-view to effectively cover all possible angles of particle incidence. No information was analyzed on the ion mass or charge state composition, and so all ions detected by Hydra are assumed to be protons. The instrument had a routine time resolution of 0.5 s to achieve an angular resolution of $\sim 16^\circ$.

Databases and Modeling

The particle environment model was constructed separately for CAMMICE/MICS data and the Hydra data. Because the multiple fields-of-view of the Hydra instrument result in nearly full coverage of all angles, the Hydra data may be easily averaged into a good representation of the omni directional flux. In contrast, the single field-of-view of the MICS sensor has good angular coverage for some intervals, but inadequate coverage at other times. This makes the construction and interpretation of the CAMMICE/MICS model more complex. The following sections describe the databases and models of the two data sets.

The NASA radiation belt models of high-energy particles are two-dimensional models, consisting of the average flux as a function of the radial magnetic coordinate L and the latitudinal coordinate B . The L coordinate is a constant for all positions along a magnetic field line and is

approximately equal to the geocentric radius of the field line where it intersects the magnetic equator. L is always given in units of Earth radii (RE). The B coordinate is the ratio of the magnetic field magnitude at the point of interest to the minimum field at the equatorial point mapped along the magnetic field line. High-energy particles such as those estimated by the NASA models form relatively symmetric azimuthal distributions. Particles of lower energy are sensitive to several effects that cause highly asymmetric populations, including electric fields and asymmetric magnetic fields. Therefore, any model of the low energy particles must be three-dimensional and use the magnetic local time as an azimuthal coordinate.

CAMMICS/MICS Model

Because of the intermittent lack of full angular coverage by MICS, the model for this data was organized by pitch angle, which is defined as the angle between the particle velocity and the local magnetic field vector. The ion flux distributions versus pitch angle were mapped to the equator and averaged into the spatial bins. Averaging over several years of the Polar mission achieved complete coverage of the equatorial pitch angle bins and provided a good representation of the average flux in most bins. Then, to obtain the omni directional flux at some latitude off the equator, the model pitch angle distributions were mapped from the equator to the latitude of interest and averaged over angle. This is equivalent to the mapping in B and L coordinates in the NASA AE8 and AP8 radiation belt models.

The raw CAMMICE/MICS data for 3.5 years were averaged into 5-minute distributions in energy and local pitch angle to build the database. The 24 energy steps from the MICS instrument were combined into 12 channels by averaging the fluxes for every other step to improve statistics. The local pitch angles for each measurement were computed using the simultaneous data from the Polar magnetic field experiment [Russell et al., 1995]. The local pitch angle distribution for each energy was averaged into 18 equally-spaced bins of 10° widths. Then the local pitch angles were converted into equatorial pitch angles using the ratio of the measured local magnetic field magnitude to the equatorial magnetic field magnitude [Schulz and Lanzerotti, 1974]. The equatorial magnetic field was calculated for this purpose using the IGRF model of the geomagnetic field. The equatorial pitch angle distribution at each energy was then averaged into spatial bins in equatorial magnetic coordinates. The magnetic equatorial plane was divided into a grid of 16 equally-spaced bins in L in the range 2–10, and 2-hour bins in magnetic local time.

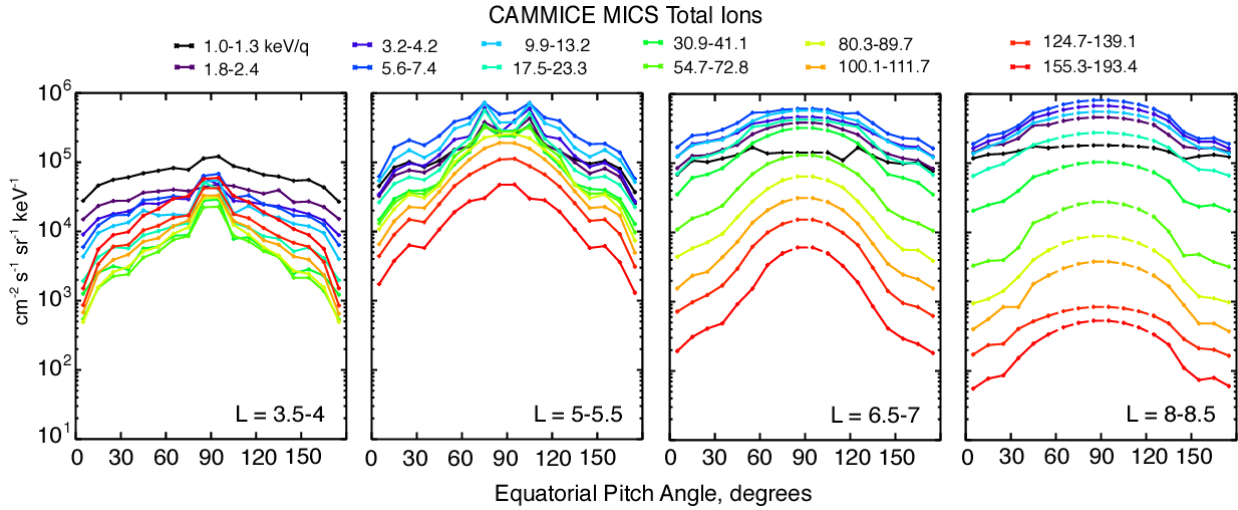


Figure 1. Average pitch angle distributions of the differential number flux of all ion species detected by the CAMMICE/MICS experiment on the Polar spacecraft. The four panels show distributions for different L bins in the 1800-2000 MLT sector.

Figure 1 shows the average pitch angle distributions of the total ion flux measured by MICS in several of the spatial bins. All twelve energy bins in the CAMMICE model are presented for each of four L bins in the dusk sector of magnetic local time. The ion energy spectrum at any given pitch angle tends to harden dramatically for the lower L bins, consistent with the adiabatic acceleration of particles. All the L bins exhibit fairly symmetric peaks at an equatorial pitch angle of 90° , which is characteristic of particles trapped in the radiation belts. The angular anisotropy, defined as the ratio of perpendicular particles to parallel particles, provides a measure of the variation of the ion flux with magnetic latitude. The anisotropy is low for the lower energy ions and increases significantly for the highest energies. This implies a substantial population of low energy ions away from the magnetic equator. The anisotropy at high L tends to be lower than that at low L for all energies. The MICS ion flux values are consistent with previously published measurements [Milillo et al., 2001].

Because of the high inclination of the Polar orbit, the coverage of the magnetic equator was lacking at high L. Polar crossed the equator at $L \sim 3$ just after launch, and the crossing point moved outward in L as the orbit precessed during the mission. At the end of 3.5 years, the magnetic equatorial crossing point had moved outward to $L \sim 5$. The ions trapped at the magnetic equator correspond in Figure 1 to the fluxes near 90° . The gap in coverage produces a corresponding gap centered at 90° , which widens in angle as L increases. Future work will include the processing of several more years of MICS data, which will increase the maximum L of the equatorial measurements.

A fitting procedure was devised to replace the missing equatorial data at high L. For each energy channel, the available data for a limited pitch angle range on either side of the gap were fitted to the standard model function $A \sin^n \alpha$ where the parameters of the fit are A, designating the flux at 90° , and n, the anisotropy index. The missing data was then filled with the model distribution using the parameter values. The limited angular range of the fitting procedure tended

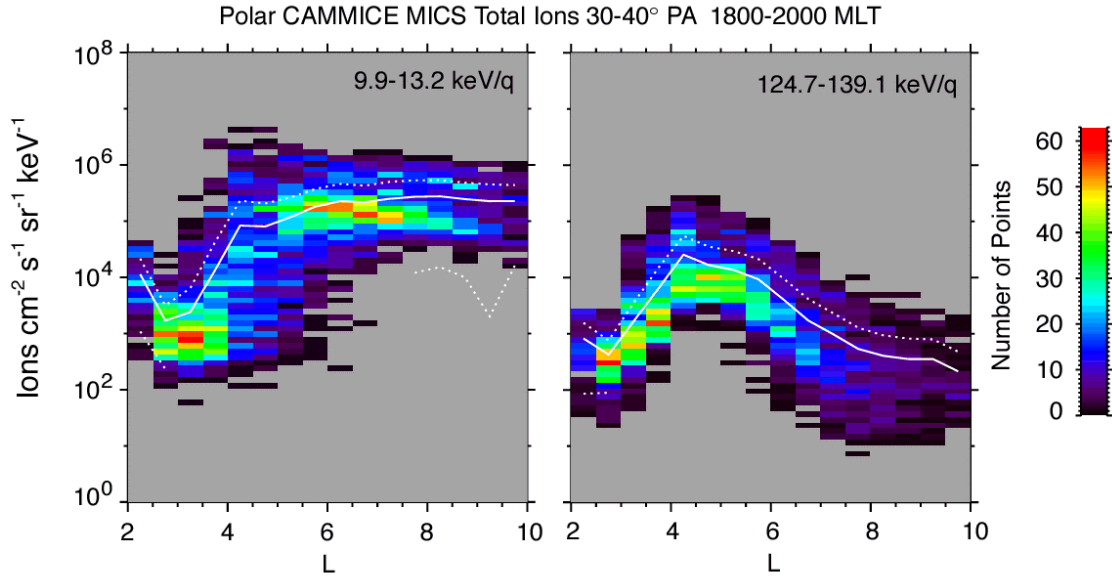


Figure 2. Statistical distribution of the total ion flux in two energy ranges for each of 16 equally-space L bins in the range 2-10. The ions shown are for the equatorial pitch angle range 30-40 in the 1800-2000 MLT sector. The solid line represents the average flux in each bin. The dotted lines mark the average flux plus and minus the standard deviation of the flux, respectively.

to preserve the character of the measured distribution. However, the fit could not compensate for the lack of measurements at the equator and so the model did not include any sharp features within the measurement gaps at 90° .

The particle flux in the Earth's magnetosphere in this interval underwent large variations. During intense geomagnetic storms the flux exceeded the quiet-time value by as much as three orders of magnitude. This is illustrated by the statistical distributions of flux shown in Figure 2. The color of each pixel in the images represents the number of MICS measurements recorded in the 3.5-year interval at a particular pitch angle for each level of flux and L. In some L bins the range of observed fluxes exceeded four orders of magnitude. To obtain a quantitative measure of this variability, standard deviations were computed for each bin of the MICS average model. The solid line in the figure represents the average flux in each bin. The dotted lines mark the average plus the standard deviation and the average minus the standard deviation of the flux, respectively. The standard deviation of the flux in each bin is typically in the range of 100–200% of the average value.

Maps of the average equatorially trapped H^+ flux are shown in Figure 3 as a function of position in the magnetic equatorial plane. These measurements correspond to the fluxes at pitch angles of 90° in the distributions shown in Figure 1. The four panels present different energy ranges of the total ion flux. The rectangular coordinates in units of Earth radii are the result of a standard polar-to-rectangular conversion of the magnetic coordinates of the bins in L and magnetic local time. The axes are oriented so that the sun is on the left side of the plot, midnight is on the right, dawn is at the top, and dusk is at the bottom, respectively. The sunlit Earth is drawn in the center of each panel for reference. The database was limited to L in the range 2–10 and so the areas outside this range were set to the color black to represent “no data.”

Figure 3 displays the expected falling spectrum with increasing energy for almost all positions, with the highest flux values at 3–4 keV and the lowest values at 155–193 keV. The maps also show that the distribution of ions in the highest energy range is relatively symmetric in local time, but the lower energy ions exhibit a pronounced enhancement in the dusk to midnight sector. At the lowest energy (3–4 keV), this dusk side bulge extends over almost the full L range. This structure is consistent with the nominal drift trajectories of low energy ions in toward the Earth from the night side and then eastward as they become energized adiabatically.

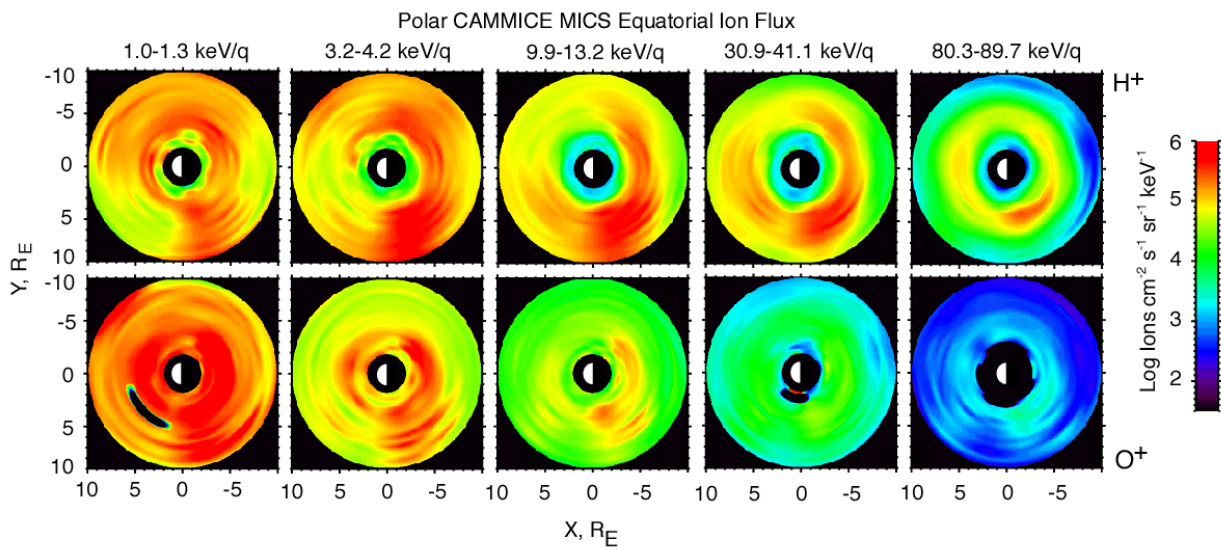


Figure 3. Average equatorially-trapped flux of H^+ and O^+ ions in five energy-per-charge ranges detected by CAMMICE/MICS plotted as a function of position in the magnetic equatorial plane.

The figure also shows maps of the equatorially-trapped O^+ ion flux as a function of position in the equatorial plane. The O^+ ions have the same spatial structures as the H^+ ions, but the energy spectrum at all locations is much softer. In the lowest energy range, the O^+ flux becomes comparable to the H^+ flux, or even dominant in some spatial bins. This figure illustrates the substantial low energy (1-5 keV) populations at $L \sim 3.5-6$ f for all local time sectors except dawn. In the midnight local time sectors these low energy components appear to extend to the outer boundary of the model at $L \sim 10$.

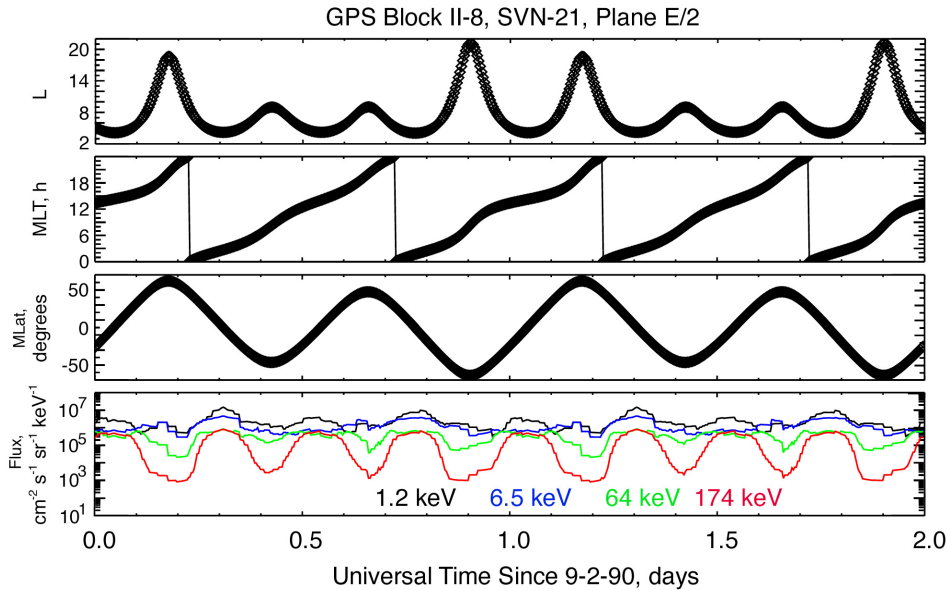


Figure 4. GPS satellite position and model H^+ flux variations for a representative two-day interval. The top three panels show the GPS satellite position in magnetic coordinates as L, magnetic local time in hours, and magnetic latitude in degrees. The bottom panel presents the average total ion flux for the GPS trajectory for four energy channels.

Hydra Model

The multiple detectors of the Hydra instrument provide full coverage of the all angles during each 6-s spacecraft spin period. So, a good estimate of the omni directional flux can be constructed by averaging the data from all detectors over any time interval longer than the spin period. The averages of the Hydra omni directional flux were averaged in a spatial grid of bins in the magnetic coordinates of L, magnetic local time, and magnetic latitude. The range and resolution of the grid are as follows: every 0.2 in L in the range 3.5–15; every 5° in magnetic latitude from -75° to 75° ; and every hour in magnetic local time in the range 0000–2400. The energy resolution and range of the Hydra instrument vary with operating mode. To aid in interpretation, the model flux spectrum in each spatial bin was interpolated to a constant set of 10 logarithmically-spaced energy channels over the range 20 eV–15 keV.

Model Average Spectra

Using the CAMMICE/MICS and Hydra models, the average environment and its variation may be estimated for a satellite in any orbit that is sufficiently covered by the model range of L and magnetic latitude. We have computed the average particle spectra for several orbits in the GPS constellation and also for a geosynchronous orbit (GEO).

To compute the average flux spectrum for a given orbit we used the following procedure. The orbital elements were used to compute the evolution of the spacecraft position in Earth Centered Inertial (ECI) coordinates. The length of the time interval was chosen to assure unbiased coverage of local time and latitude. The time resolution of the position was selected to provide

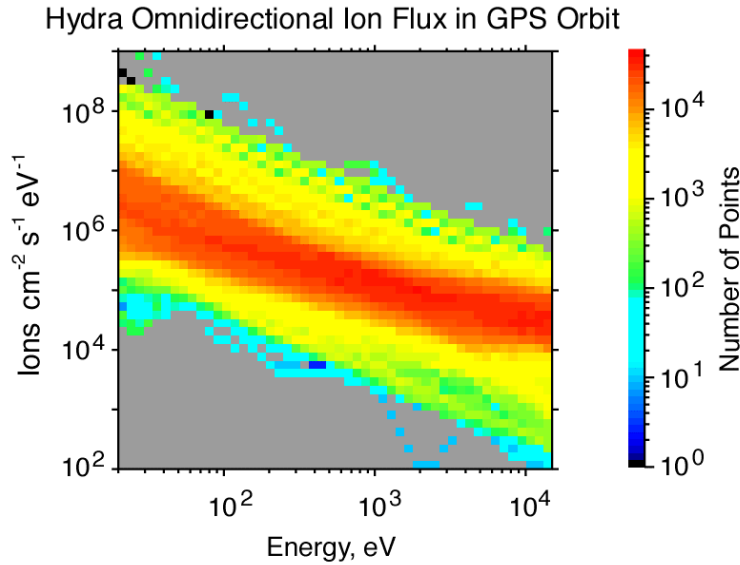


Figure 5. Ion flux measurements by the Hydra instrument on the Polar satellite averaged over the trajectory of a GPS satellite for a one-year interval.

spatial resolution comparable to, or finer than the particle models. For the GPS and GEO cases, we used 1-year intervals with the satellite position computed each minute.

The spacecraft ECI position and the Universal Time were used to compute the satellite position in the magnetic coordinates of L, magnetic latitude, and magnetic local time. These coordinates are then used to determine the model bin specifying the flux at that position. The omni directional flux spectrum at each position of the satellite was then obtained by a query to the Hydra model. The average spectrum over the orbit is the mean of these spectra at all the positions over the 1-year interval.

The CAMMICE/MICS model, in contrast to the Hydra model, is specified at the magnetic equator and these fluxes must be mapped to the satellite latitude to estimate the local environment. Such a mapping along the magnetic field line may be performed using only the ratio of the magnetic field magnitudes at the two locations. The IGRF empirical geomagnetic field model was employed to calculate the magnetic field magnitude at the satellite to the field magnitude at magnetic equator along the same field line. With the ratio of these two field magnitudes, we converted the average equatorial pitch angle distribution at each energy in the specified bin to the pitch angle distribution locally at the satellite latitude. The omni directional flux spectrum was then calculated by integrating the distributions over all local pitch angles for each energy channel. The omnidirectional spectrum was then averaged over all positions of the satellite, similar to the Hydra data.

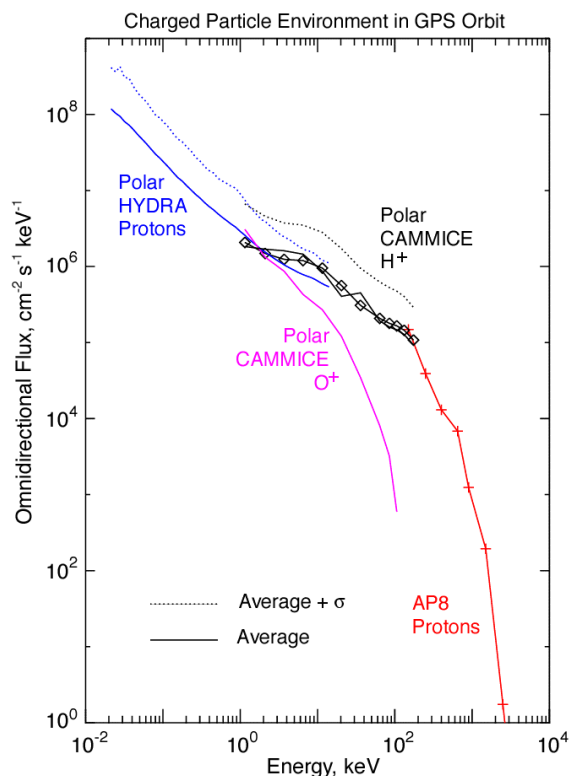


Figure 6. Average model omnidirectional differential number flux spectra of several species of ions experienced by a GPS spacecraft. Solid lines mark the average flux and dotted lines represent the average plus the standard deviation of the flux, respectively.

Figure 4 shows a portion of the data from the calculation of the orbital-averaged environment for the case of the GPS mission. This particular case is for the trajectory of the GPS Block II-8, SVN-21 in orbital plane E/2. The top three panels present the position of a GPS satellite in the magnetic coordinates of L, magnetic local time in hours, and magnetic latitude in degrees for an arbitrary 2-day interval. The satellite trajectory covered a range of $\pm 70^\circ$ in magnetic latitude and $L \sim 3\text{--}21$. All local times are covered and the magnetic equatorial crossings occur near the times of the minimums in L. The bottom panel shows the average total ion fluxes at four energies given by the CAMMICE/MICS model for these positions. At all energies the flux tended to maximize during the equatorial crossings and decreased at times when the satellite is at high values of L. The CAMMICE/MICS model covered the range $L \sim 2\text{--}10$ and we have chosen to set the flux for all positions for $L > 10$ to the model flux value at the outer boundary of $L \sim 10$. The flux at the outer boundary tended to be low and so this approximation does not affect significantly the orbital average. The orbital variation was almost three orders of magnitude at high energies and much less at the low energy channels.

The results of the Hydra orbital average calculation are shown in Figure 5. The plot displays the statistical variation of the ion spectrum as a function of energy in the range 20 eV–14 keV. The color of each pixel in the images represents the number of Hydra measurements recorded for each level of flux and energy. Due to the high time resolution of the Hydra instrument, the number of points for each energy is quite high. The relative standard deviation of the flux are in the range of $\sim 100\text{--}200\%$, similar to the statistics of the CAMMICE/MICS data.

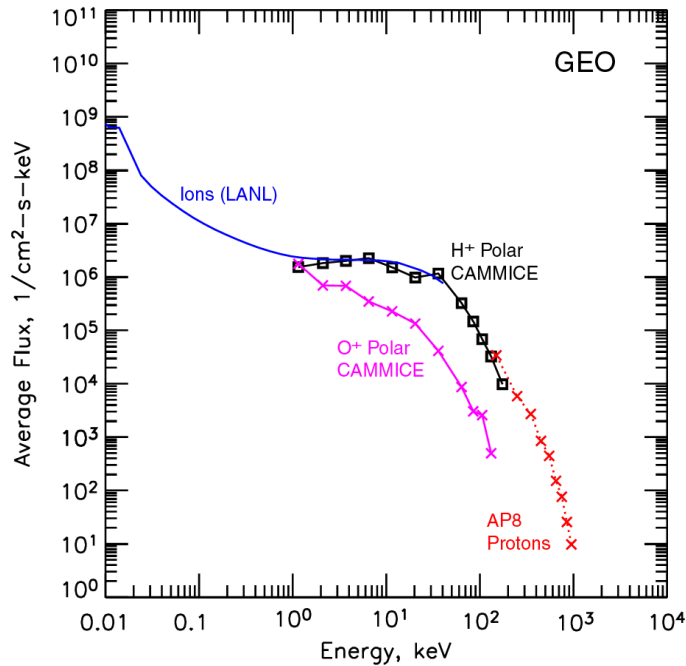


Figure 7. Average model omnidirectional differential number flux spectra of ions and electrons experienced by a spacecraft in geosynchronous orbit.

Figure 6 presents a summary of the model results for the particle environment in GPS orbit. The average omnidirectional flux spectra from the CAMMICE/MICS and Hydra models are compared with the output of the NASA radiation belt models. The solid lines represent the average flux and the dotted lines mark the sum of the average plus the standard deviation of the flux for each species. The color of the plotted lines identify the measured particle species: Hydra protons as a blue line, CAMMICE/MICS total ions as a black diamonds, CAMMICE/MICS H^+ as a black line, and CAMMICE/MICS O^+ as a magenta line. The protons from the NASA AP8 model averaged over the same orbit are plotted as a red line with crosses.

The plotted CAMMICE/MICS model spectrum for H^+ ions overlays the total ion spectrum within the limitations of statistics. This demonstrates that H^+ is the dominant ion species excepting energies of ~ 1 keV. The average ion flux spectrum measured by Hydra agrees with the CAMMICE/MICS result within a factor of two in the overlapping energy range of 1–14 keV. The NASA AP8 model provided an average spectrum of protons for energies of 100–3000 keV which is plotted as red crosses in the figure. It fits smoothly with the CAMMICE/MICS spectrum of H^+ ions at 100 keV. So we have constructed a reasonable estimate of the average ion proton flux spectrum in the GPS orbit over six orders of magnitude in energy. The dotted lines mark the sum of the average and the standard deviation of the flux from the CAMMICE/MICS and Hydra instruments. This provides an estimate of the flux variation averaged over the GPS trajectory.

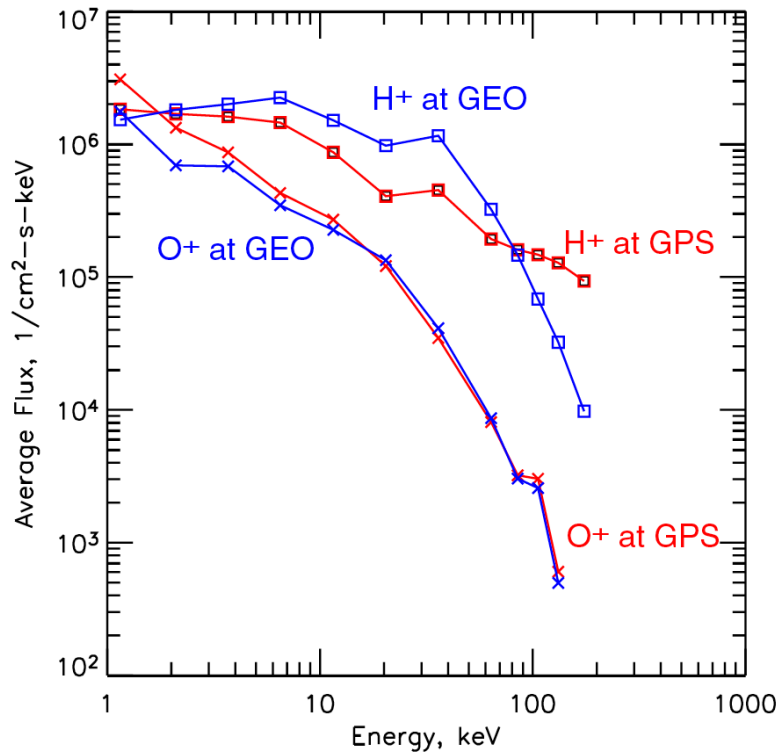


Figure 8. Average model omnidirectional differential number flux spectra of ions and electrons experienced by a spacecraft in geosynchronous and GPS orbit.

Figure 6 also shows that O^+ flux plotted in magenta becomes comparable to the H^+ flux at energy of 1–2 keV. At energy below 1 keV the oxygen ion flux is uncertain because the Hydra measurements cannot distinguish between different ion species. Similar calculations for other GPS orbital planes and phases exhibit differences of $\sim 2\%$ from these results.

The CAMMICE/MICS model has also been used to estimate the average particle environment of spacecraft in geosynchronous orbit (GEO). Figure 7 shows a summary of the average particle spectrum for GEO. The CAMMICE/MICS spectra are compared with the low energy ions and electrons from the LANL empirical model [Korth et al., 1999]. The LANL model was constructed using the data from the Magnetospheric Plasma Analyzer (MPA) on several geosynchronous spacecraft. The LANL model provides the ion flux at energies in the range 10 eV–31 keV as a function of the planetary magnetic index K_p , but with no mass or charge state information. The average ion spectrum at GEO was computed from the LANL model using the statistical distribution of K_p during 1996. Figure 7 shows that the LANL average ion spectrum matches the CAMMICE/MICS H^+ spectrum to within 50%. The CAMMICE/MICS H^+ spectrum also coincides very well with the proton estimate from AP8. The electron flux at from the LANL model matches the AE8 flux at 40 keV within a factor of two, but the slope of the spectrum is discontinuous at that energy.

Figure 7 also presents the CAMMICE/MICS average flux of O^+ ions for GEO as red crosses. It is not very different from the average O^+ spectrum in GPS orbit. This point is illustrated by

Figure 8, which compares the CAMMICE/MICS H⁺ and O⁺ average flux spectra for the two orbits. The GPS averages are plotted in red and the GEO averages are shown in blue.

Summary

A three-dimensional model of the average ion environment in the energy range 1–200 keV was constructed from 3.5 years of data from the CAMMICE/MICS instrument on the NASA Polar satellite. The model provides the average H⁺ and O⁺ ion flux as a function of energy and pitch angle for any equatorial spatial position in the range $L \sim 2-10$ and all magnetic local times. Using a magnetic field model, the angular distributions may be mapped to any magnetic latitude in the range $\pm 70^\circ$. The mapped fluxes can then be integrated over all angles to obtain the omnidirectional ion flux spectrum as a function of the three-dimensional position in space. We have averaged the ion flux over GPS and geosynchronous orbits resulting in an estimate of the average ion environment for a satellite in those orbits.

For the case of the GPS orbit, the CAMMICE/MICS model has been compared to a similar model of six years of Hydra ion measurements in the energy range 0.02–14 keV. The Hydra model provides the average total omnidirectional ion flux as a function of energy for spatial position. The Hydra ion spectra were averaged over the GPS orbit for comparison to the CAMMICE/MICS model. Excellent agreement between the two models was achieved in the overlap energy range 1–14 keV. The average ion spectra in GEO estimated from the CAMMICE/MICS model also compared favorably with the average ion flux derived from the model of Korth et al. [1999].

At high energies the CAMMICE/MICS average ion spectra in GEO and GPS orbits was compared with estimates of the proton flux from the NASA AP-8 model. Good agreement was achieved between the models in the energy range 100–200 keV. Combining all the above models made possible an unprecedented estimate of the ion environment from 20 eV to 3 MeV.

At high energies (~ 100 keV) the flux estimates agree with corresponding estimates from the NASA AP-8 model, but the fluxes at low energies are larger than those extrapolated simply from AP-8. The CAMMICE/MICS model shows that H⁺ dominates the >2 keV ion populations, but that the O⁺ flux becomes comparable to the H⁺ flux at ~ 1 keV. The standard deviation of both the ion and electron flux was found to be 100–200% of the average value over the entire considered energy range. The average 1–200 keV O⁺ flux estimates for GEO appear very similar to the averages for GPS orbit, so that any material damage due to O⁺ ions should be the same for the two orbits.

Acknowledgements

The authors thank C. T. Russell for the use of the data from the Magnetic Field Investigation on the NASA Polar satellite. The work at The Aerospace Corporation was supported under grant number GC131165NGD from Boston University.

References

1. Acuna, M. H., K. W. Ogilvie, D. N. Baker, S. A. Curtis, D. H. Fairfield, and W. H. Mish, The global geospace science program and its investigations, *Space Sci. Rev.* 71, 5-21, 1995.
2. Blake, J. B., J. F. Fennell, L. M. Friesen, B. M. Johnson, W. A. Kolasinski, D. J. Mabry, J. V. Osborn, S. H. Penzin, E. R. Schnauss, H. E. Spence, D. N. Baker, R. Belian, T. A. Fritz, W. Ford, B. Laubscher, R. Stiglich, R. A. Baraze, M. F. Hilsenrath, W. L. Imhof, J. R. Kilner, J. Mobilia, D. H. Voss, A. Korth, M. Gull, K. Fisher, M. Grande, D. Hall, CEPPAD, *Space Sci. Rev.*, 71, 531-562, 1995.
3. Hastings, D., and H. Garrett, *Spacecraft-Environment Interactions*, Cambridge University Press, Cambridge, United Kingdom, 1996.
4. Johnson, R. E., *Energetic Charged-Particle Interactions with Atmospheres and Surfaces*, Springer-Verlag, Berlin, Germany, 1990.
5. Kistler, L. M., F. M. Ipavich, D. C. Hamilton, G. Gloeckler, B. Wilken, G. Kremser, and W. Studemann, Energy spectra of the major ion species in the ring current during geomagnetic storms, *J. Geophys. Res.*, 94, 3579-3599, 1989.
6. Koga, R., S. S. Imamoto, N. Katz, S. D. Pinkerton, Data processing units for eight magnetospheric particle and field sensors, *J. Spacecraft and Rockets*, 29, 574-579, 1992.
7. Korth, H., M. F. Thomsen, J. E. Borovsky, and D. J. McComas, Plasma sheet access to geosynchronous orbit, *J. Geophys. Res.*, 104, 25047-25061, 1999.
8. Milillo et al., An empirical model of the ion distributions in the equatorial inner magnetosphere, *Phys. Chem. Earth*, 24, 209-214, 1999.
9. Milillo et al., Empirical model of proton fluxes in the equatorial inner magnetosphere: development, *J. Geophys. Res.*, 106, 25713-5729, 2001.
10. Nastasi, M., J. W. Mayer, and J. K. Hirvonen, *Ion-solid interactions: fundamentals and applications*, Cambridge University Press, Cambridge, United Kingdom, 1996.
11. Russell, C. T., R. C. Snare, J. D. Means, D. Pierce, D. Dearborn, M. Larson, G. Barr, and G. Le, The GGS/Polar magnetic fields investigation, *Space Sci. Rev.*, 71, 563-582, 1995.
12. Schulz, M., and L. J. Lanzerotti, *Particle Diffusion in the Radiation Belts*, Springer-Verlag, Berlin, Germany, 1974.

13. Scudder, J., F. Hunsacker, G. Miller, J. Lobell, T. Zawistowski, K. Ogilvie, J. Keller, D. Chornay, F. Herrero, R. Fitzenreiter, D. Fairfield, J. Needell, D. Bodet, J. Googins, C. Kletzing, R. Torbert, J. Vandiver, R. Bentley, W. Fillius, C. McIlwain, E. Whipple, and A. Korth, Hydra-a 3-dimensional electron and ion hot plasma instrument for the polar spacecraft of the GGS mission, *Space Sci. Rev.*, 71, 459-495, 1995.
14. Vette, J. J., The NASA/National Space Science Data Center Trapped Radiation Model Program (1964-1991), NSSDC World Data Center A for Rockets and Satellites, Report Number 91-29, November 1991.
15. Wilken, B., W. Weiss, D. Hall, M. Grande, F. Sorass, J. F. Fennell, Magnetospheric ion composition spectrometer onboard the CRRES spacecraft. *J. Spacecraft and Rockets*, 29 585-591, 1992.